<Supporting Information>

Synthesis, characterization, and photoluminescence properties of three two-dimensional lanthanide-containing Dawson-type polyoxometalates†

Hechen Wu†, Minna Zhi†, Chunli Chen, Yanhong Zhu, Pengtao Ma*, Jingping Wang and Jingyang Niu*

Henan Key Laboratory of Polyoxometalate Chemistry, College of Chemistry and Chemical Engineering, Henan University, Kaifeng, Henan 475004, P. R. China

Materials and Methods. All reagents used were of analytical grade and obtained from commercial sources without further purification. $Na_{12}[P_2W_{15}O_{56}]\cdot 24H_2O$ was prepared according to the literature and conformed by IR spectroscopy. Elemental analyses of C, H, and N were performed with an Elementar VarioElcube CHNS analyzer. IR spectroscopy were recorded on a Bruker VERTEX 70 IR spectrometer using KBr pellets in the range of 4000-400 cm^{-1}. PXRD data were obtained on a Bruker AXS D8 Advance diffraction meter with Cu Kα radiation (λ = 1.5418 Å) at room temperature. The TGA curves were performed under flowing N_2 atmosphere using a Mettler-Toledo TGA/SDTA 851e heat analysis meter with a heating ratio of 10 °C min^{-1} from 25 to 800 °C. Raman spectra were performed on a Renishaw in Via with a red Spectra-Physics He-Ne laser (wavelength of 532 nm and 500 mW capacity). The UV/vis diffuse reflectance spectra and UV absorption spectra were performed on a UH4150 UV-vis spectrometer.

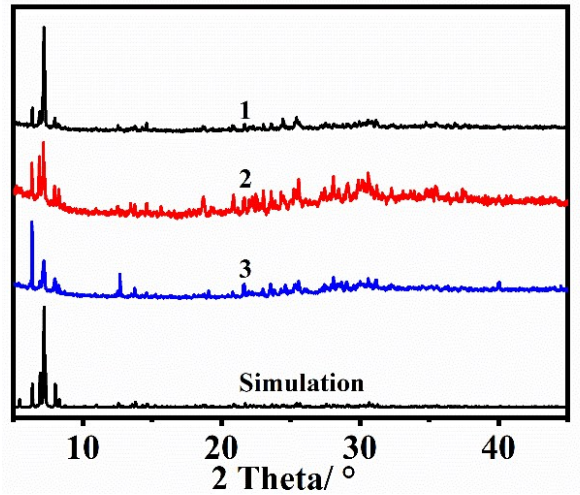

Fig. S1. The experimental and simulated PXRD patterns of **1**–**3**.

Table S1 selected bond length of **1**–**3**

La–O	Bond length (Å)	Ce–O	Bond length (Å)	Pr–O	Bond length (Å)
La1-O1W	2.60(3)	Ce1-O27	2.54(2)	Pr1-O27	2.48(3)
La1-O2W	2.61(3)	Ce1-O28	2.52(3)	Pr1-O28	2.49(3)
La1-O3W	2.57(4)	Ce1-O33	2.52(4)	Pr1-O33	2.48(4)
La1-O4W	2.76(4)	Ce1-O40	2.43(3)	Pr1-O40	2.45(3)
La1-O27	2.52(3)	Ce1-O64	2.63(4)	Pr1-O64	2.70(3)
La1-O28	2.50(3)	Ce1-O1W	2.58(4)	Pr1-O1W	2.54(5)
La1-O33	2.53(3)	Ce1-O2W	2.55(4)	Pr1-O2W	2.49(5)
La1-O40	2.48(3)	Ce1-O3W	2.55(4)	Pr1-O3W	2.52(4)
La1-O64	2.61(3)	Ce1-O4W	2.66(5)	Pr1-O4W	2.63(5)
La2-O5W	2.63(3)	Ce2-O16	2.62(3)	Pr2-O16	2.57(3)

La2-O6W	2.62(4)	Ce2-O76	2.49(3)	Pr2-O76	2.45(4)
La2-O7W	2.64(3)	Ce2-O79	2.45(3)	Pr2-O79	2.41(3)
La2-O16	2.58(3)	Ce2-O83	2.46(3)	Pr2-O83	2.43(4)
La2-O76	2.50(3)	Ce2-O87	2.37(4)	Pr2-O87	2.38(4)
La2-O79	2.44(3)	Ce2-O5W	2.56(5)	Pr2-O5W	2.60(5)
La2-O83	2.48(3)	Ce2-O6W	2.57(5)	Pr2-O6W	2.60(5)
La2-O87	2.43(3)	Ce2-O7W	2.54(4)	Pr2-O7W	2.55(5)
La3-O4	2.55(3)	Ce3-O4	2.55(3)	Pr3-O4	2.57(3)
La3-O8W	2.46(5)	Ce3-O17	2.53(3)	Pr3-O17	2.54(3)
La3-O9W	2.55(4)	Ce3-O8W	2.43(5)	Pr3-O8W	2.49(5)
La3-O10W	2.56(4)	Ce3-O9W	2.57(4)	Pr3-O9W	2.52(4)
La3-O11W	2.51(5)	Ce3-O10W	2.54(4)	Pr3-O10W	2.47(5)
La3-O12W	2.42(4)	Ce3-O11W	2.62(4)	Pr3-O11W	2.52(4)
La3-O13W	2.46(4)	Ce3-O12W	2.44(3)	Pr3-O12W	2.42(4)
La3-O14W	2.59(3)	Ce3-O13W	2.47(4)	Pr3-O13W	2.45(3)
La3-O17	2.49(3)	Ce3-O14W	2.54(3)	Pr3-O14W	2.58(4)
Average	2.542 (4)	Average	2.528 (4)	Average	2.513 (4)

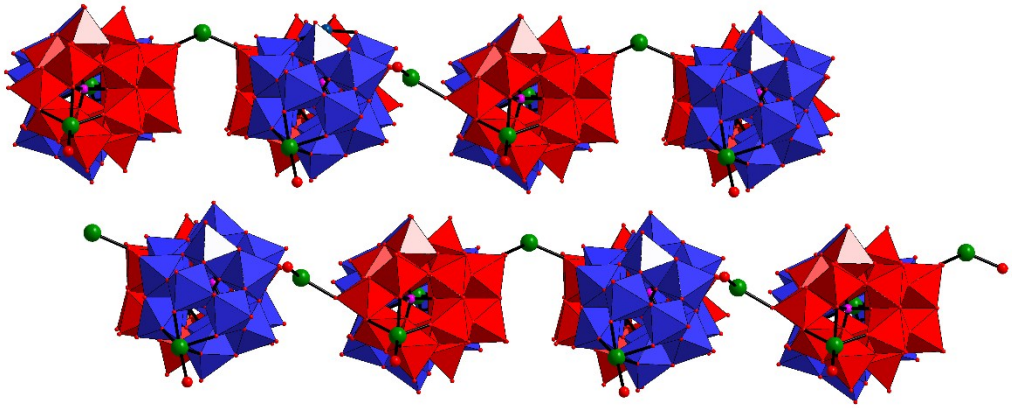

Fig. S2. The packing arrangement of 2D network architecture of **1**.

Table S2 BVS results of Ce ions in **2**

	BVS
Ce1	3.07
Ce2	3.23
Ce3	3.34

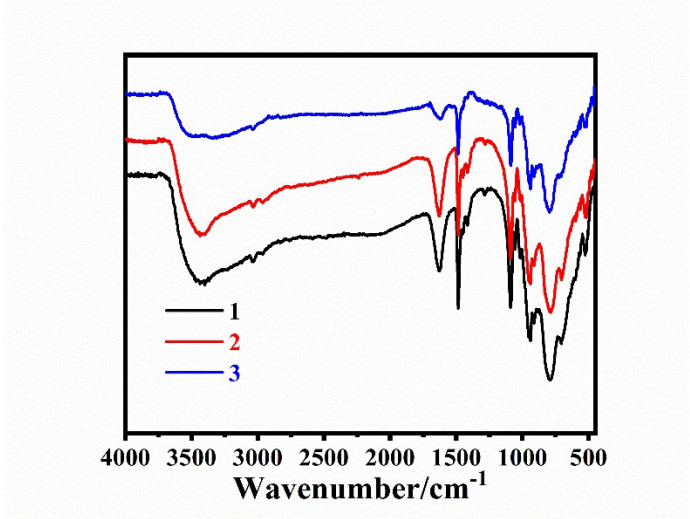

Fig. S3 IR spectroscopy of **1–3**.

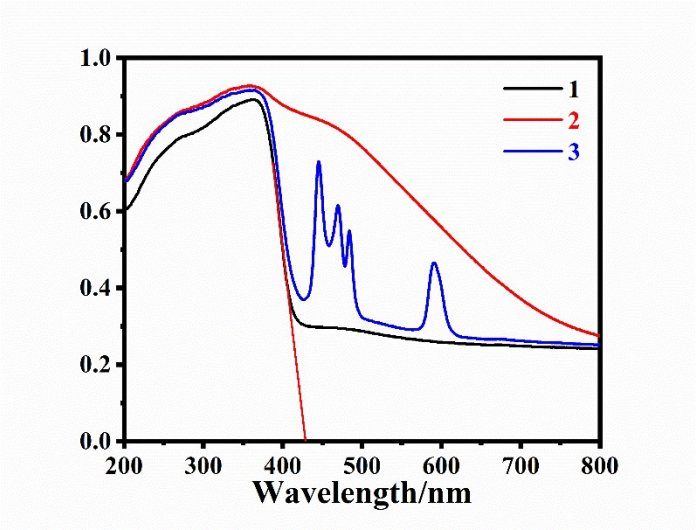

Fig. S4 The UV absorption spectra of **1–3**.

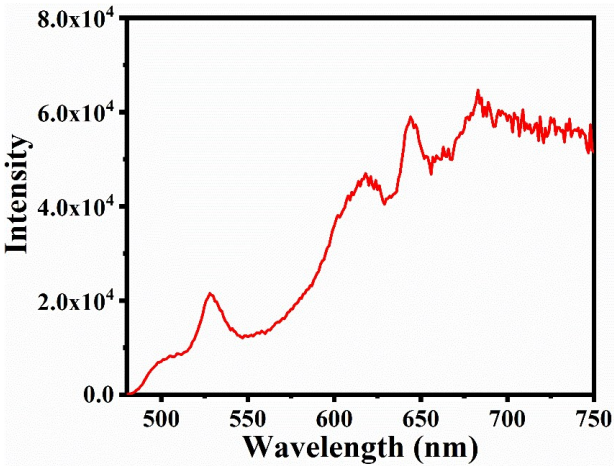

Fig. S5. The emission spectra of **1** (λ_{ex} = 448 nm).

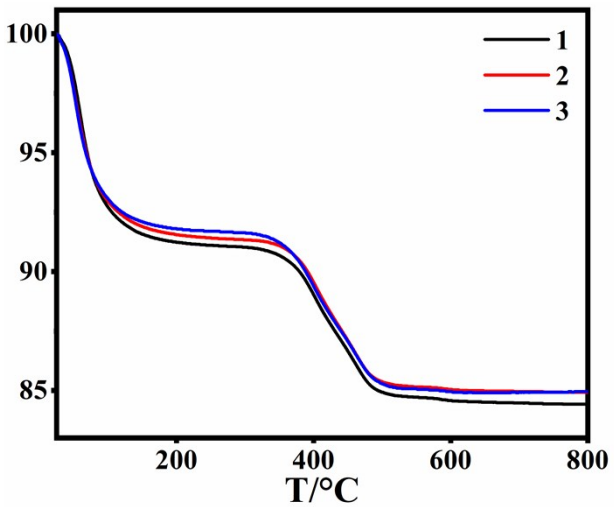

Fig. S6. TGA curves of **1**–**3**.

As shown in Fig. S6, the similar TGA curves of compound **1**–**3** show two steps of weight loss from 25 °C to 800 °C. In detail, the first experimental loss of 8.57% can be assigned to the loss of forty-eight lattice water (Cal. 8.53%), and the second experimental loss of 6.49% can be attributed to the loss of fourteen coordination water, three $[N(CH_3)_4]^+$ cations, and partial decompose of POM skeleton.